

Ballistic side jump motion of electrons and holes in semiconductor quantum wells

John Schliemann

Institute for Theoretical Physics, University of Regensburg, D-93040 Regensburg, Germany

(October 6, 2018)

We investigate the ballistic motion of electrons and holes in III-V semiconductor quantum wells with spin-orbit coupling and a homogeneous in-plane electric field. As a result of a non-perturbative treatment of both of these influences, particle wave packets undergo a pronounced side jump perpendicular to the field direction. For wave packets of sufficient width the amplitude of this motion can be estimated analytically and increases with decreasing field strength. We discuss the scaling behavior of the effect and some of its experimental implications.

Effects of spin-orbit coupling in semiconductors have become a particularly lively direction of solid-state research. Most of the activities here are embedded in the emerging field of spintronics. An early paradigm of this area is the spin field-effect transistor proposed by Datta and Das over fifteen years ago [1]. In this device proposal, electrons are injected from a spin-polarized source electrode into a quantum well in which the dominant contribution to spin-orbit interaction is given by the Rashba coupling,

$$\mathcal{H}_R = \frac{\alpha}{\hbar} (p_x \sigma^y - p_y \sigma^x). \quad (1)$$

Here \vec{p} is the momentum of the electron confined in a two-dimensional geometry, and $\vec{\sigma}$ the vector of Pauli matrices. The Rashba coefficient α is tunable by an electric gate across the well and can therefore be varied experimentally [2]. As a result, in the course of the electron's ballistic motion through the quantum well its spin undergoes a controlled rotation which can be detected by another spin-polarized drain electrode. To enable the injection of electrons into this device, a certain voltage has to be applied between source and drain electrode, leading to a possibly small but nevertheless finite in-plane electric field in the quantum well. In the present letter we investigate the effect of such an electric field in combination with spin-orbit coupling. As we shall see below, the interplay between spin-orbit coupling and an in-plane electric field adds an important feature to the ballistic electron dynamics: The electron performs a side-jump motion perpendicular to the direction of the electric field. The field here is assumed to be homogeneous, in contrast to side jump motion upon scattering on impurities which is discussed intensively in circumstances of the anomalous Hall effect [3].

Moreover, as it was pointed out recently, spin-orbit coupling of the type (1) does not only lead to a rotation of the spin, but has also an effect on the orbital degree of freedom: the electron performs a *zitterbewegung*, i.e. an oscillatory motion superimposed on the nonrelativistic dynamics of the particle wave packet [4]. In the absence of an electric field the single-particle Hamiltonian reads $\mathcal{H} = \frac{\vec{p}^2}{2m} + \mathcal{H}_R$ where m is the effective band mass.

In this case a fully analytical description of the *zitterbewegung* can be given in terms of the time-dependent position operator $\vec{r}_H(t) = \exp(i\mathcal{H}t/\hbar)\vec{r}(0)\exp(-i\mathcal{H}t/\hbar)$ in the Heisenberg picture. As we shall see, the side jump phenomena to be discussed below are accompanied by *zitterbewegung* of this type.

Another important recent development regarding spin dynamics in semiconductors is the prediction of the intrinsic spin Hall effect [5–8]. This effect is again a consequence of spin-orbit coupling and amounts in a spin current (as opposed to a charge current) driven by a perpendicular electric field. Therefore, this situation is similar to the Datta-Das transistor with the electric field being provided by the source-drain voltage. Here spin orbit coupling of the Rashba type has the peculiarity that the spin Hall conductivity vanishes in an infinite system in the presence of any spin relaxation mechanism [9]. However, this conclusion holds only in the thermodynamic limit, and for a device of mesoscopic size and sufficient carrier mobility, spin Hall transport signaled by spin accumulation at the sample edges should be considered as possible.

Let us consider an electron in an n-doped quantum well being subject to Rashba spin-orbit coupling and a constant in-plan electric force \vec{F} , i.e. the single-particle Hamiltonian reads $\mathcal{H} = \frac{\vec{p}^2}{2m} + \mathcal{H}_R - \vec{F}\vec{r}$. Thus, the time-dependent momentum operator is given by $\vec{p}_H(t) = \vec{p}(0) + \vec{F}t$, while the spin operators fulfill the equations

$$\frac{d}{dt}\sigma_H^x(t) = \frac{2\alpha}{\hbar^2}p_H^x(t)\sigma_H^z(t), \quad (2)$$

$$\frac{d}{dt}\sigma_H^y(t) = \frac{2\alpha}{\hbar^2}p_H^y(t)\sigma_H^z(t), \quad (3)$$

$$\frac{d}{dt}\sigma_H^z(t) = -\frac{2\alpha}{\hbar^2}[p_H^x(t)\sigma_H^x(t) + p_H^y(t)\sigma_H^y(t)] \quad (4)$$

with $\vec{\sigma}_H(0) = \vec{\sigma}$. Note that the position operator \vec{r} does not occur in the above equations, and therefore the time-dependent spin operators $\vec{\sigma}_H(t)$ can be formulated as a function of the zero-time Schrödinger operators \vec{p} , $\vec{\sigma}$ only. In particular, when the operators $\vec{\sigma}_H(t)$ are applied on eigenstates of the momentum $\vec{p} = \vec{p}(0)$, the quantities $\vec{p}_H(t) = \vec{p}(0) + \vec{F}t$ become real numbers, ren-

dering Eqs. (2)-(4) as an system of ordinary differential equations for the 2×2 -matrices $\vec{\sigma}_H(t)$. Unfortunately an explicit analytical solution of these equations for general directions of the force \vec{F} and the initial momentum $\vec{p}(0)$ does not seem to be possible. However, such a solution can be given if \vec{F} and $\vec{p}(0)$ are collinear. Since the Rashba Hamiltonian (1) is invariant under rotations of spin and momentum in the xy-plane, we can choose, without loss of generality, \vec{F} and $\vec{p}(0)$ to point along the x -direction where we find

$$\sigma_H^x(t) = \sigma^x \cos\left(\frac{2\alpha}{\hbar^2}\left(p^x t + \frac{1}{2}Ft^2\right)\right) + \sigma^z \sin\left(\frac{2\alpha}{\hbar^2}\left(p^x t + \frac{1}{2}Ft^2\right)\right), \quad (5)$$

$$\sigma_H^y(t) = \sigma^y, \quad (6)$$

$$\sigma_H^z(t) = -\sigma^x \sin\left(\frac{2\alpha}{\hbar^2}\left(p^x t + \frac{1}{2}Ft^2\right)\right) + \sigma^z \cos\left(\frac{2\alpha}{\hbar^2}\left(p^x t + \frac{1}{2}Ft^2\right)\right). \quad (7)$$

Note that the argument of the trigonometric functions is the integral $\int_0^t dt' p_H^x(t')$, generalizing the situation without an external field and therefore constant momentum.

The time-dependent position operators $\vec{r}_H(t)$ fulfill the equations

$$\frac{d}{dt}x_H(t) = \frac{p_H^x(t)}{m} + \frac{\alpha}{\hbar}\sigma_H^y(t), \quad (8)$$

$$\frac{d}{dt}y_H(t) = \frac{p_H^y(t)}{m} - \frac{\alpha}{\hbar}\sigma_H^x(t). \quad (9)$$

Let us now consider the expectation values $\langle \vec{r}_H(t) \rangle$ for an initial state with momentum $\vec{p} \parallel \vec{F}$ along the x -direction, spin in positive z -direction and $\langle \vec{r}_H(0) \rangle = 0$. Here we have $\langle x_H(t) \rangle = (p^x t + \frac{1}{2}Ft^2)/m$, and the y -component reads

$$\langle y_H(t) \rangle = -\frac{\alpha}{\hbar} \int_0^t dt' \sin\left(\frac{2\alpha}{\hbar^2}\left(p^x t' + \frac{1}{2}Ft'^2\right)\right). \quad (10)$$

If the initial spin direction is reversed, $\langle y_H(t) \rangle$ changes sign. The case of vanishing initial momentum $\vec{p}(0) = 0$ is particularly interesting. Here the physical problem contains only two length scales which are conveniently chosen as the Rashba length $\lambda_R = \hbar^2/m\alpha^2$ and the field-dependent length $l_F = \sqrt{\alpha/F}$. The latter quantity determines the amplitude of the side jump motion to be discussed now. Figure 1 shows a plot of $\langle y_H(t) \rangle$ for $\vec{p}(0) = 0$, $F = 1.0\text{meV}/\mu\text{m}$, and a band mass $m = 0.023m_0$, corresponding to the conduction band mass on InAs, where m_0 is the bare electron mass. The Rashba parameter has been fixed to $\alpha = 0.01\text{eVnm}$ which is a realistic value for InAs [8]. The main panel shows the a real-space plot of $\langle \vec{r}_H(t) \rangle$ with the time t ranging from zero to $t = 50\text{ps}$. One can clearly distinguish two phases

of the electron motion: In a first phase with $\langle x_H(t) \rangle \lesssim 200\text{nm}$, the transverse expectation value $\langle y_H(t) \rangle$ starts at $\langle y_H(0) \rangle = 0$ and undergoes a pronounced monotonic side jump motion to $|\langle y_H(t) \rangle| \approx 60\text{nm}$. In a following second phase $\langle y_H(t) \rangle$ performs a *zitterbewegung*, i.e. an oscillatory motion around this value with its amplitude decreasing with increasing longitudinal distance $\langle x_H(t) \rangle$. The period of the *zitterbewegung* as a function of $\langle x_H(t) \rangle$ is approximately given by $\pi\lambda_R \approx 1040\text{nm}$ [4]. The inset of figure 1 shows the same data for $\langle y_H(t) \rangle$ but as a function of time t . After a time interval of $t = 50\text{ps}$ the electron wave number is $k^x(t) = p^x(t)/\hbar = Ft/\hbar < 0.08\text{nm}^{-1}$ which is still close to the Γ -point in III-V semiconductors. Thus, the assumptions underlying the effective-mass approximation and the Rashba Hamiltonian (1) are perfectly valid.

As seen from figure 1, the magnitude of the side jump can be obtained by performing the formal limit

$$\lim_{t \rightarrow \infty} \langle y_H(t) \rangle = -\frac{\alpha}{\hbar} \int_0^\infty dt \sin\left(\frac{\alpha}{\hbar^2}Ft^2\right) \quad (11)$$

$$= -l_F \sqrt{\frac{\pi}{8}}, \quad (12)$$

where we have used the integral $\int_0^\infty dt \sin(t^2) = \sqrt{\pi/8} \approx 0.62$. For the above parameters we have $l_F = 100\text{nm}$ corresponding to a side jump of about 62nm , in perfect agreement with the numerical plot. Note that according to Eq. (10) the band mass m does not enter the function $\langle y_H(t) \rangle$, but is inversely proportional to $\langle x_H(t) \rangle$. Thus, changing the effective mass as $m \mapsto m'$ amounts in a rescaling of the abscissa in the main panel of figure 1 by a factor of m/m' . Thus the above considerations relating to InAs are trivially extended to other materials, say GaAs. In the latter case the Rashba coupling is typically somewhat smaller which can be compensated by a smaller in-plane field F , resulting the the same length scale l_F , i.e. the same magnitude of side jump.

In the above discussion we have concentrated on plane-wave eigenstates of the momentum. However, a localized electron in a quantum well is not described realistically by a single plane wave but rather a superposition of them. We therefore consider a Gaussian wave packet,

$$\langle \vec{r} | \psi \rangle = \frac{1}{2\pi\sqrt{\pi}} \int d^2k e^{-\frac{1}{2}d^2(\vec{k}-\vec{k}_0)^2} e^{i\vec{k}\vec{r}} \begin{pmatrix} 1 \\ 0 \end{pmatrix}, \quad (13)$$

where the initial spin direction is again along the z -axis. We numerically solve for the dynamics of such a wave packet by superimposing plane-wave solutions whose initial momenta have been chosen from a grid centered around \vec{k}_0 in reciprocal space. Because the in-plane field \vec{F} is in general not collinear with such initial momenta, these plane-wave solutions have also to be generated numerically. Moreover, in such a procedure necessarily requires a wave vector cutoff. In all numerical simulations

to be presented below we have carefully checked that the data is well-converged with respect to grid spacing and wave vector cutoff.

For simplicity, let us concentrate again on the case of zero initial group wave number, $\vec{k}_0 = 0$. Then the width d of the wave packet is the only new length entering the problem. Figure 2 shows numerical simulations of the real space dynamics for different wave packet width d with otherwise the same parameters as before, $l_F = 100\text{nm}$. As seen from the figure, the dynamics of a single plane wave discussed in Eqs. (10), (12) is a good approximation to the wave-packet motion if $d \gg l_F$. In fact, for $d = 1000\text{nm} = 10l_F$ the dynamics of the wave packet is very close to the plane-wave result shown in figure 1, which continues to be a good approximation up to $d \approx 500\text{nm} = 5l_F$, whereas for smaller d the nature of the motion clearly changes. The criterion $d \gg l_F$ follows from the observation that Eqs. (2)-(4) are invariant under the rescaling $\vec{F} \mapsto q\vec{F}$, $\vec{p} \mapsto \sqrt{q}\vec{p}$, $t \mapsto t/\sqrt{q}$ with q being a real parameter. Therefore, in order to ensure invariance, the width d of the wave packet has to scale as d/\sqrt{F} which uniquely determines $l_F = \sqrt{\alpha/F}$ as the relevant length scale. Note also that Eqs. (2)-(4) are also invariant under the replacements $(p_H^i(t), \sigma_H^i(t)) \mapsto (-p_H^i(t), -\sigma_H^i(t))$, $i \in \{x, y\}$. As a consequence, for the above situation of a wave packet symmetric around its group wave vector $\vec{k}_0 = 0$ and the force \vec{F} pointing along the x -direction, we have the scaling behavior $\langle y_H(t) \rangle \mapsto \langle y_H(t) \rangle / \sqrt{q}$, whereas $\langle x_H(t) \rangle$ remains unchanged. The latter conclusions hold for any symmetric wave packet, independently of its form and width; in particular, the magnitude of the side jump scales always the same way as l_F . Analogous findings hold for the rescaling $\alpha \mapsto q\alpha$, $\vec{p} \mapsto \vec{p}/\sqrt{q}$, $t \mapsto t/\sqrt{q}$ leading to $\langle x_H(t) \rangle \mapsto \langle x_H(t) \rangle / \sqrt{q}$, $\langle y_H(t) \rangle \mapsto \sqrt{q}\langle y_H(t) \rangle$. Therefore, figure 2 is of universal character since data for other values of α , F can be obtained by a simple rescaling of the coordinate axes.

So far we have concentrated on the Rashba Hamiltonian (1) as an effective contribution to spin orbit coupling. The situation is changed only marginally if the Rashba coupling is replaced with the Dresselhaus term [10] in its linear approximation [11]. When both terms are present an analytical solution for $\vec{\sigma}_H(t)$ does not appear to be possible even for initial conditions with $\vec{p}(0) \parallel \vec{F}$. An exception is the case when the Dresselhaus and the Rashba term are equal in magnitude: Here side jump and *zitterbewegung* are absent because of an additional conserved quantity arising at this high-symmetry point [12].

Let us now turn to p-doped quantum wells of III-V semiconductors. Here the low-energy physics is dominated by the heavy holes, and the spin-orbit interaction term analogous to the Rashba coupling on electron spins reads [13]

$$\tilde{\mathcal{H}}_R = i \frac{\tilde{\alpha}}{2\hbar^3} (p_-^3 \sigma_+ - p_+^3 \sigma_-), \quad (14)$$

using the notations $p_{\pm} = p_x \pm ip_y$, $\sigma_{\pm} = \sigma^x \pm i\sigma^y$. The Pauli matrices operate on the total angular momentum states with spin projection $\pm 3/2$ along the growth direction chosen as then z -axis, and $\tilde{\alpha}$ is the spin-orbit coupling coefficient. This Hamiltonian contains two length scales which are, similarly to the previous case of conduction-band electrons, aptly chosen to be the field-dependent length $\tilde{l}_F = (\tilde{\alpha}/F)^{1/4}$ and the Rashba length $\tilde{\lambda}_R = m\tilde{\alpha}^2/\hbar^2$ where m is the effective heavy-hole band mass. Moreover, an analytical plane-wave solution can again be found if the initial momentum $\vec{p}(0)$ is collinear with the in-plane force \vec{F} . Choosing this direction, again without loss of generality, to lie along the x -axis, one finds

$$\begin{aligned} \sigma_H^x(t) &= \sigma^x \cos\left(\frac{2\tilde{\alpha}}{\hbar^4} \int_0^t dt' (p^x + Ft')^3\right) \\ &\quad - \sigma^z \sin\left(\frac{2\tilde{\alpha}}{\hbar^4} \int_0^t dt' (p^x + Ft')^3\right), \end{aligned} \quad (15)$$

$$\sigma_H^y(t) = \sigma^y, \quad (16)$$

$$\begin{aligned} \sigma_H^z(t) &= \sigma^x \sin\left(\frac{2\tilde{\alpha}}{\hbar^4} \int_0^t dt' (p^x + Ft')^3\right) \\ &\quad + \sigma^z \cos\left(\frac{2\tilde{\alpha}}{\hbar^4} \int_0^t dt' (p^x + Ft')^3\right), \end{aligned} \quad (17)$$

where the remaining integral is elementary. For a plane-wave state with $\vec{p}(0) = 0$, $\langle \vec{r}_H(0) \rangle = 0$ one finds again $\langle x_H(t) \rangle = Ft^2/2m$ and

$$\langle y_H(t) \rangle = -\frac{3\tilde{\alpha}}{\hbar^3} \int_0^t dt' (Ft')^2 \sin\left(\frac{\alpha}{2\hbar^4} F^3 t'^4\right). \quad (18)$$

The magnitude of the side jump is given by the limit

$$\begin{aligned} \lim_{t \rightarrow \infty} \langle y_H(t) \rangle &= -3 \cdot 2^{3/4} \left(\frac{\tilde{\alpha}}{F}\right)^{1/4} \int_0^{\infty} dx x^2 \sin(x^4) \\ &\approx -1.428 \cdot \tilde{l}_F. \end{aligned} \quad (19)$$

Thus, the length scale \tilde{l}_F plays a similar role as l_F for conduction-band electrons. Moreover, analogously to this previous case, the behavior of plane-wave states is mimicked by proper wave packets provided $d \gg \tilde{l}_F$, a conclusion following from similar scaling arguments as before. The situation is illustrated in figure 3 with numerical simulations for values for m , $\tilde{\alpha}$ appropriate for heavy holes in p-doped GaAs quantum wells and $\tilde{l}_F = 10\text{nm}$. For wave packet width up to $d \approx 5\tilde{l}_F$ the magnitude of the side jump is quantitatively well described by Eq. (19), whereas for smaller values of d the nature of the dynamics changes.

In summary, the pronounced side jump found in the dynamics of electrons and holes in semiconductor quantum wells is the non-perturbative effect of the interplay of spin-orbit coupling and a homogeneous electric

field. The magnitude of the side jump motion is governed by the field-dependent length scales $l_F = \sqrt{\alpha/F}$ and $\tilde{l}_F = (\tilde{\alpha}/F)^{1/4}$ for electrons and holes, respectively, provided that the width d of the particle wave packet being initially at rest fulfills $d \gtrsim 5(l_F, \tilde{l}_F)$. A possible scenario for the experimental detection of the side jump effect are two opposite quantum point contacts of width d whose centers are displaced by $\Delta \approx 0.2d$. The conductivity of this setup should be maximal if the experimentally tunable parameters α ($\tilde{\alpha}$) and F are adjusted such that $l_F(\tilde{l}_F) \approx \Delta$.

Another interesting question is the connection between the ballistic side jump motion and the intrinsic spin Hall effect in diffusive systems. In a heuristic but appealing picture one can interpret spin hall transport as iterated side jumps occurring during the ballistic motion between scattering events. In fact a theoretical synthesis of extrinsic and intrinsic mechanisms of spin Hall transport [8] was put forward in Ref. [14] where the side jump contribution to the spin Hall conductivity was found to be independent of disorder and particle interactions.

I thank I. Adagideli and D. Weiss for useful discussions. This work was supported by the SFB 689 ‘‘Spin Phenomena in reduced Dimensions’’.

[1] S. Datta and B. Das, Appl. Phys. Lett. **56**, 665 (1990).
[2] E. I. Rashba, Fiz. Tverd. Tela (Leningrad) **2**, 1224 (1960) (Sov. Phys. Solid State **2**, 1109 (1960)); Y. A. Bychkov and E. I. Rashba, J. Phys. C **17**, 6039 (1984).
[3] For a historical overview see J. Sinova, T. Jungwirth, and J. Cerne, Int. J. Mod. Phys. B **18**, 1083 (2004).
[4] J. Schliemann, D. Loss, and R. M. Westervelt, Phys. Rev. Lett. **94**, 206801 (2005); Phys. Rev. B **73**, 085323 (2006).
[5] S. Murakami, N. Nagaosa, and S. C. Zhang, Science **301**, 1348 (2003).
[6] J. Sinova, D. Culcer, Q. Niu, N. A. Sinitsyn, T. Jungwirth, and A. H. MacDonald, Phys. Rev. Lett. **92**, 126603 (2004).
[7] J. Schliemann and D. Loss, Phys. Rev. B **71**, 085308 (2005).
[8] J. Schliemann, Int. J. Mod. Phys. B **20**, 1015 (2006).
[9] This result was obtained first by J. I. Inoue, G. E. W. Bauer, and L. W. Molenkamp, Phys. Rev. B **70**, 041303 (2004), studying spin Hall transport in the presence of static impurities within a diagrammatic expansion. For further developments and generalizations of this conclusion see Ref. [8].
[10] G. Dresselhaus, Phys. Rev. **100**, 580 (1955).
[11] M. I. Dyakonov and V. Y. Kachorovskii, Sov. Phys. Semicond. **20**, 110 (1986); G. Bastard and R. Ferreira, Surf. Science **267**, 335 (1992).
[12] J. Schliemann, J. C. Egues, and D. Loss, Phys. Rev. Lett. **90**, 146801 (2003).

[13] R. Winkler, Phys. Rev. B **62**, 4245 (2000); L. G. Gerchikov and A. V. Subashiev, Sov. Phys. Semicond. **26**, 73 (1992).
[14] E. M. Hankiewicz, G. Vignale, and M. Flatte, condmat/0603144.

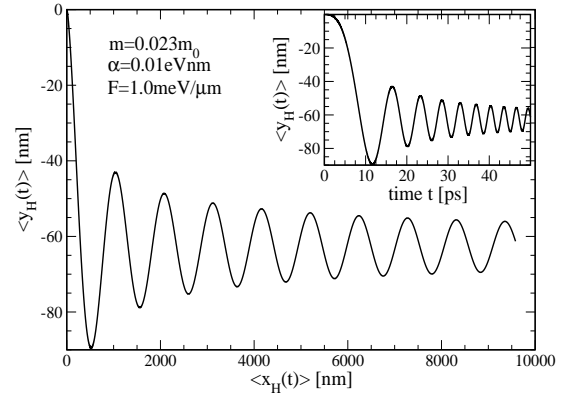


FIG. 1. Main panel: real-space motion $\langle \vec{r}_H(t) \rangle$ for a plane wave with $\vec{p}(0) = 0$. The inset shows $\langle y_H(t) \rangle$ as a function of time t .

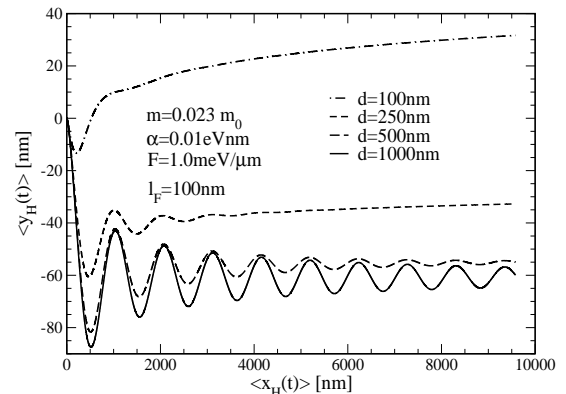


FIG. 2. Real-space motion $\langle \vec{r}_H(t) \rangle$ for electron wave packets with zero initial group velocity and different width d .

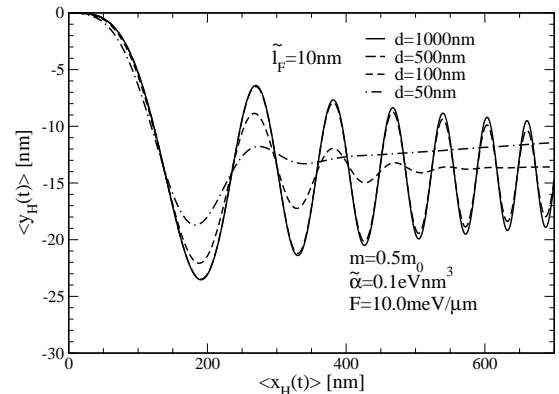


FIG. 3. Real-space motion $\langle \vec{r}_H(t) \rangle$ for hole wave packets with zero initial group velocity and different width d .